GDCh Research Article Angewandte International Edition Chemie www.angewandte.org

How to cite: *Angew. Chem. Int. Ed.* **2025**, *64*, e202420243
doi.org/10.1002/anie.202420243

Photomechanical Crystals Hot Paper

Distinctive Photomechanical Shape Change of *p*-Phenylenediacrylic Acid Dimethyl Ester Single Crystals Induced by a Spatially Heterogeneous Photoreaction

Daichi Kitagawa, Rei Tomoda, Sebastian A. Ramos, Gregory J. O. Beran,* Christopher J. Bardeen, and Seiya Kobatake**

Abstract: Understanding photoreaction dynamics in crystals is important for predicting the dynamic property changes accompanying these photoreactions. In this work, we investigate the photoreaction dynamics of *p*-phenylenediacrylic acid dimethyl ester (***p*-PDAMe**) in single crystals that show reaction front propagation, in which the photoreaction proceeds heterogeneously from the edge to the center of the crystal. Moreover, we find that ***p*-PDAMe** single crystals exhibit a distinctive crystal shape change from a parallelogram to a distorted shape resembling a fluttering flag, then to a rectangle as the photoreaction proceeds. Density functional theory calculations predict the crystal structure after the photoreaction, providing a reasonable explanation of the distinctive crystal shape change that results from the spatially heterogeneous photoreaction. These results prove that the spatially heterogeneous photoreaction dynamics have the ability to induce novel crystal shape changes beyond what would be expected based on the equilibrium reactant and product crystal shapes.

Introduction

Molecules that change their chemical structures in response to external stimuli have been investigated for applications such as switches, sensors, and actuators.[1] In particular, photoresponsive molecules can be used for the photomechanical materials that can directly convert photon energy into macroscopic work.[2] Solid-state photomechanical materials typically consist of photoresponsive molecules organized inside liquid-crystalline polymers,[3] amorphous or semicrystalline polymers,[4] gels,[5] or single crystals.[6] Among these materials, single crystals have typically shown superior actuator performance such as fast response speeds, high energy densities, and reasonable photon-to-work-conversion efficiencies.[7] Previous studies on photomechanical crystals have reported various mechanical responses, including expansion, contraction, bending, twisting, peeling, oscillation, rolling, and jumping.[8] One goal of the field is to generate novel shape changes that go beyond these deformations. A second goal is to clarify the relationship between the nanoscale changes in molecular structure and packing accompanying photoreaction and micro/macroscopic photomechanical response. This is often accomplished by using X-ray crystallographic analysis. On larger scales, illumination conditions,[9] crystal morphology,[10] and crystal size[11] are also key factors that determine the mode of photomechanical response because they can affect the mechanical strain tensor induced by the photochemical reactions.

In addition to the factors above, we hypothesize that photoreaction dynamics in crystals also play an important role in their photomechanical response. Photoreaction dynamics in crystals can give rise to novel effects such as reaction front propagation. For example, we found that the photochemical reaction of 2,5-distyrylpyrazine (DSP) in single crystals proceeds spatially heterogeneously from the edge to the center of the crystal on length scales that can be resolved by optical microscopy, typically on the order of 1 micron.[12] Furthermore, we recently showed that the [4+4] photodimerization of 9-cyanoanthracene (9CA) and 9-anthraldehyde (9AA) in single crystals also proceeds from the edge to the center of the crystal, while the photodimerization of 9-methylanthracene and 9-acethylanthracene proceeds homogeneously throughout the crystal.[13] Detailed investigation revealed that surface effects, in which the reactivity of the crystal surface is much higher than that of the crystal interior, and positive cooperative effects, in which the photoproducts promote the reaction of the remaining reactants, are necessary to observe spatially heterogeneous photoreactions, and these effects are closely related to the amount of molecular rearrangement required for the reaction to occur in the crystal lattice. Although the observation of spatially heterogeneous reaction dynamics depends on the molecule studied, the presence of a reaction front has so far not given rise to a qualitatively different photomechanical response. In both heterogeneous and homogeneous reacting crystals, only smooth expansion in the horizontal direction was observed. Note that changes in

[*] D. Kitagawa, R. Tomoda, S. Kobatake
Department of Chemistry and Bioengineering, Graduate School of Engineering, Osaka Metropolitan University, 3-3-138 Sugimoto, Sumiyoshi-ku, 558-8585 Osaka, Japan
E-mail: kitagawa@omu.ac.jp
kobatake@omu.ac.jp

S. A. Ramos, G. J. O. Beran, C. J. Bardeen
Department of Chemistry, University of California, Riverside, 501 Big Springs Road, 92521 Riverside, CA, USA
E-mail: gregory.beran@ucr.edu

the thickness were not measured in these experiments. It is an open question as to whether spatially heterogeneous reaction dynamics can give rise to novel photomechanical responses, like the generation of irregular shapes.

In this work, we focus on the photochemical reaction of *p*-phenylenediacrylic acid dimethyl ester (***p*-PDAMe**) in single crystals. Similar to DSP, ***p*-PDAMe** molecules undergo a photopolymerization reaction in the crystalline state (Figure 1a).[14] Observation of ***p*-PDAMe** single crystals by a hyperspectral camera confirms that the photochemical reaction proceeds spatially heterogeneously from the edge to the center of the crystal. However, the different unit cell orientation in ***p*-PDAMe** single crystals allows them to undergo a distinctive sequence of photomechanical shape changes. The crystal starts as a parallelogram but then distorts to a shape resembling a fluttering flag as the ends are converted to a different unit cell. As the reaction proceeds, this shape transformation propagates to the crystal center, finally transforming it into a rectangle. Density functional theory calculations reveal the molecular packing changes induced by the photoreaction, and these changes can be directly associated with the microscopic shape change. By turning off the light at any point, the crystal can be frozen into one of these shapes, providing a wide range of photoinduced shape changes that extend beyond what would be expected based on the reactant and product crystal shapes.

Results and Discussion

To prepare single crystals for investigating both photoreaction kinetics and photomechanical effects, we tried several crystal growth methods and found that casting a toluene solution containing ***p*-PDAMe** onto a glass slide afforded plate-like crystals with a thickness less than 1 μm as shown in Figures 1b and S1. The details of the preparation method are described in the Supporting Information. To determine the molecular orientation in the crystal, powder X-ray diffraction (PXRD) measurements were performed. Figure S2 shows PXRD pattern of the plate-like crystal and the pattern calculated from single-crystal X-ray crystallographic data reported previously (a triclinic crystal system and a space group of $P\bar{1}$).[15] Only diffraction peaks corresponding to the (110) or (−1−10) Miller planes were observed for the plate-like crystals, suggesting that the horizontal surface corresponds to either the (110) or (−1−10) face. Figure 1c shows an enlarged optical microphotograph of the plate-like crystal. The corner angles of the crystal were 75° and 105°. Figure 1d illustrates the ideal crystal shape viewed from the (−1−10) face based on the data of X-ray crystallographic analysis. The calculated corner angles in the illustration are 75° and 105°, in good agreement with the actual crystal shape, indicating that the structure of the plate-like crystals is the same as that reported previously.[15] Figure 1e shows the molecular packing viewed from the (−1−10) face. Note that only molecules in the same layer are drawn for clarity, and the black cell indicates the minimum repeating unit of the molecular arrangement that determines the crystal shape. Thus, the plate-like crystals of ***p*-PDAMe** were fully characterized.

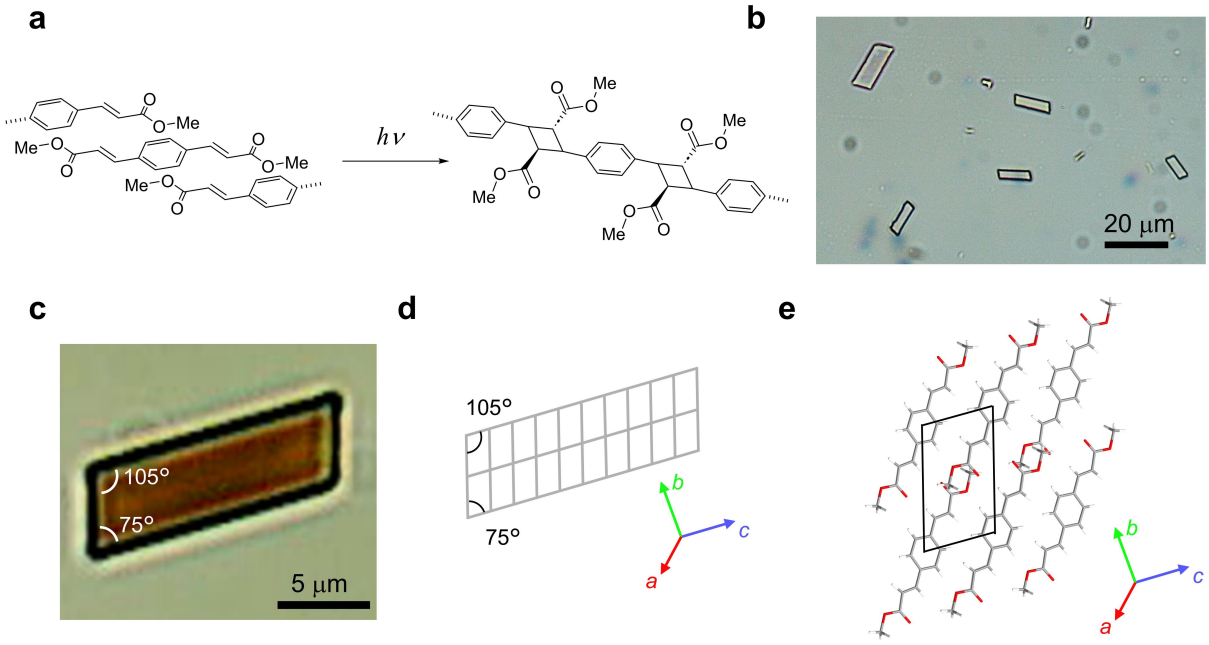

Figure 1. (a) Photopolymerization reaction of ***p*-PDAMe**, (b, c) optical microphotographs of ***p*-PDAMe** single crystals prepared by the casting method, (d) ideal crystal shape viewed from the (−1−10) face based on X-ray crystallographic data, and (e) molecular packing in the crystal viewed from the (−1−10) face.

To follow the progress of photoreactions in the single crystal of ***p*-PDAMe**, the transmission spectra at various points during the photoreaction were measured under parallel Nicols. Birefringence measurements were performed because ***p*-PDAMe** molecules do not absorb in the visible light region. Figure 2a shows the crystal shape of ***p*-PDAMe** and the locations of the areas where the intensity of transmitted light was measured using a hyperspectral camera. As shown in Figure S3, in all areas, the transmitted light intensity increased with increasing the irradiation time of UV (365 nm) light, and the spectral shapes before and after photoreaction are very similar, indicating that the photopolymerization reaction proceeded in the same way in all areas, although there seemed to be differences in the reaction rates. To compare the reaction rate in each area, the change in the intensity of transmitted light relative to the irradiation time was transformed to the change in the conversion ratio as shown in Figure 2b. The detailed procedures are described in our previous work.[12] As can be seen, the change in the conversion ratio showed a sigmoidal curve and increased in the order of Area 1, Area 2, and Area 3, indicating that the photoreaction proceeded spatially heterogeneously from the edge to the center of the crystal, as seen for DSP, 9CA, and 9AA.[12–13] This is due to the combination of enhanced surface reactivity and a positive cooperative effect, in which the initially formed photoproduct facilitates reaction of adjacent crystal regions. Thus, we could confirm the spatially heterogeneous photoreaction in ***p*-PDAMe** single crystals.

Next, we investigated the photomechanical response of ***p*-PDAMe** single crystals. Figure 3 and Movie S1 show the shape change of ***p*-PDAMe** single crystals upon UV irradiation observed under parallel Nicols. Upon UV irradiation, the transmitted light color changed from brown to colorless, starting from the short sides of the crystals due to the spatially heterogeneous photoreaction. This is likely due to the positive cooperative effect and the surface effect. Namely, the photoreaction is initiated at the crystal edges

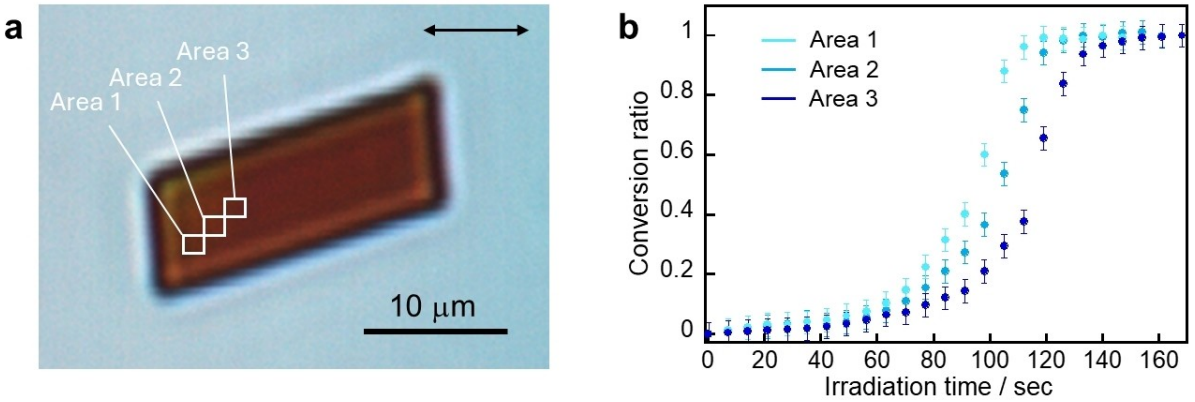

Figure 2. (a) Optical microphotograph of ***p*-PDAMe** single crystals observed under parallel Nicols and locations of areas where the transmission spectra were measured. The directions of the polarizer and analyzer are depicted as the black arrow. (b) Change in the conversion ratio relative to the irradiation time of 365 nm light (9.95 mW cm^{-2}) calculated from the change in the transmitted light intensity at 500 nm.

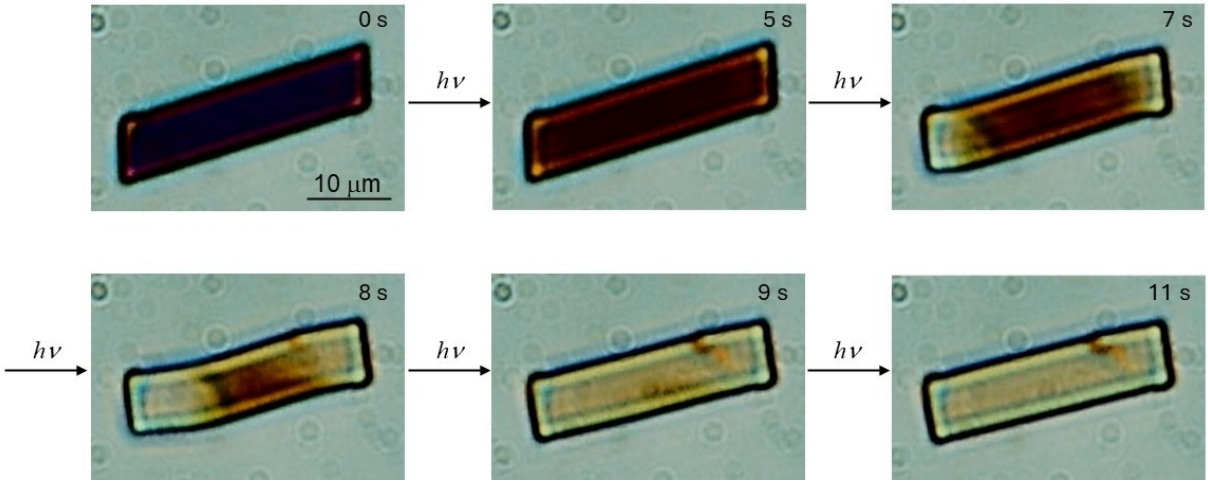

Figure 3. Photomechanical shape change of ***p*-PDAMe** single crystal upon irradiation with 365 nm light (59.7 mW cm^{-2}) observed under parallel Nicols. The directions of the polarizer and analyzer are horizontal.

due to the surface effect, then propagates toward the center of the crystal due to the cooperative effect. The photoreaction propagates preferentially along the long axis of the crystal. We hypothesize that this anisotropic propagation is due to the fact that the distance between molecules along the long axis of the crystal is shorter than that along the short axis of the crystal, as can be seen in Figure 1e, resulting in a stronger cooperative effect. Although this is one plausible explanation, further studies are needed, including quantitative evaluation and theoretical modelling of the anisotropy of the photochemical reaction front propagation.

Very interestingly, the anisotropic reaction front propagation changed the crystal shape from a parallelogram to a distorted shape resembling a fluttering flag, then to a rectangle as the photoreaction proceeded. This unique photomechanical shape change has been confirmed to be reproducible in other crystals, as shown in Movie S2. Figure S4 shows the changes in the crystal dimensions (the length of the short and long sides and thickness) before and after the photoreaction. It was found that the length of the long side slightly decreases (ca. −0.6 %), while there was no detectable change in the length of the short side and the thickness direction of the crystal. Moreover, by ceasing the UV irradiation, the crystal shape change could be stopped, and the "flag" shape remained its shape even after 16 hours (Figure S5). In other plate-like crystals studied previously, the reaction did not induce a discontinuity in the crystal shape because the photoreaction proceeded homogeneously across the crystal. For instance, a single crystal of 1,2-bis(2-ethyl-5-phenyl-3-thienyl)perfluorocyclopentene changed continuously from a square shape to a lozenge shape.[6a] Here, the photoreaction proceeds spatially heterogeneously, with reacted and unreacted regions coexisting in different regions within a single crystal, leading to the distinctive photomechanical shape change. Furthermore, to confirm that this photomechanical shape change was due to a single-crystal-to-single-crystal transformation, the crystallinity after the photoreaction was checked under crossed Nicols. As shown in Figure S6, the sample exhibited birefringence even after the photoreaction, indicating that crystallinity was retained after the photoreaction.

To understand the distinctive crystal shape change at the molecular level, we focused on the change in the molecular packing. Nakanishi et al. previously performed X-ray crystallographic analysis of ***p*-PDAMe** crystals before and after the photoreaction.[14] In that study, they could not determine the detailed crystal structure after the photoreaction but did obtain information about the change in the unit cell dimensions using a partially photoreacted crystal. We also tried to perform X-ray crystallographic analysis of larger photoreacted crystals. Unfortunately, these efforts were unsuccessful because numerous cracks were generated in these crystals as the photoreaction progressed, as shown in Figure S7 and Movie S3. These fractured crystals were not suitable for X-ray analysis. Therefore, we attempted to elucidate the molecular packing change after the photoreaction with the help of periodic density functional theory (DFT) calculations performed with the dispersion-corrected B86bPBE-XDM density functional. Using our recently-established topochemical approach,[16] which has successfully predicted photochemical transformations in several other organic crystals, we predicted the crystal structure of the polymer photoproduct by replacing the molecules in the reactant crystal structure with the photoreacted species. The product species were positioned so as to minimize the atomic displacements between the reactants and product, and the atomic positions were then relaxed with DFT. Next, the crystal lattice parameters were changed to match the experimentally-reported values of the photoproduct crystal, and the atomic positions were again relaxed (with unit cell parameters held constant) to obtain the final predicted ***p*-PDAMe** photoproduct structure.

Figure S8 shows the molecular packing after photopolymerization of ***p*-PDAMe** as determined by DFT calculations constrained by the unit cell parameters reported experimentally. To confirm the validity of the molecular packing obtained by the DFT calculations, the PXRD pattern of the structure generated by the DFT calculations was compared with that obtained experimentally. Figure S9 shows the change in the experimental PXRD pattern upon UV irradiation. The initial pattern before UV irradiation is in good agreement with the simulated pattern calculated from X-ray crystallographic data (Figure S9a and b). After the prolonged UV irradiation, the pattern changes substantially due to the photoreaction and becomes similar to the pattern simulated from the DFT-predicted structure although there are slight differences (Figure S9c and d). These results indicate that we have successfully predicted the molecular packing of the photoproduct through the combination of DFT calculations and knowledge of the experimental lattice parameters. Crystallographic data for the reactant and product crystal structures are summarized in Table S1.

The DFT-predicted structural transformation provides insight into the mechanism of the distinctive photomechanical shape change. Figure 4a shows the change in the minimum repeating unit of the molecular arrangement in a layer before and after the photoreaction viewed from the (−1−10) face. Accompanying the photoreaction, it was found that the minimum repeating unit of the molecular arrangement changes from a parallelogram to a rectangle. In addition, the length of the short edge of the minimum repeating unit expands from 5.844 Å to 6.040 Å (ca. +3.3 %), while the long edge contracts from 9.822 Å to 9.678 Å (ca. −1.5 %). The change of the thickness is also depicted in Figure S10. The distance between molecular layers decreases from 5.503 Å to 5.448 Å (ca. −1.0 %). Concerning the crystal shape change mentioned above, only the shrinkage of the long side of the crystal cannot be explained based on the change in the minimum repeating unit. Presumably, this is because the unit cell dimensions used in the DFT calculations come from the partially reacted crystal data, and are slightly different from the real ones, as observed in the discrepancies in the peak positions of the PXRD patterns. However, we emphasize that the change in the minimum repeating unit predicted by DFT calculations can provide a qualitative mechanism for the distinctive photomechanical shape change. Figure 4b illustrates a plau-

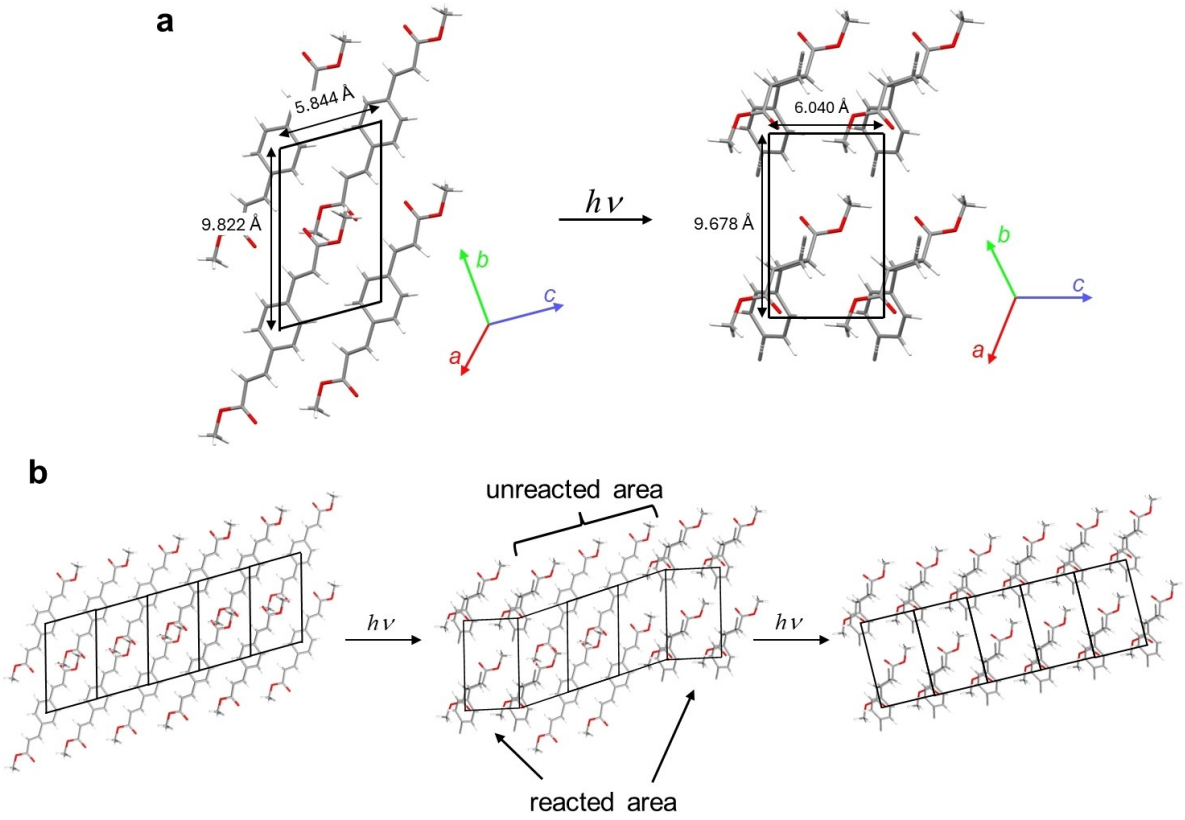

Figure 4. (a) Change in the molecular packing and the minimum repeating unit of the molecular arrangement of ***p*-PDAMe** crystal before and after the photoreaction viewed from the (−1−10) face. Note that only molecules (or parts of polymers) in the same layer are drawn for clarity, and the black cell indicates the minimum repeating unit of the molecular arrangement. (b) Plausible mechanism of the distinctive photomechanical shape change.

sible mechanism of the sequential photomechanical shape changes of ***p*-PDAMe** single crystals. The photoreaction is initiated near the crystal edges, where the molecules' larger free volumes lead to higher reactivity. Then, as the molecules at the edges react and undergo structural rearrangements, the free space increases around the interior molecules. This increased free space facilitates the reactivity of the interior molecules in a positive cooperative manner. As a result, the photoreaction proceeds spatially heterogeneously from the edge to the center of the crystal. Meanwhile, the minimum repeating unit of the molecular arrangement also changes from a parallelogram to a rectangle shape. During the photoreaction, reacted and unreacted regions coexist in different regions of the same crystal. In the reacted regions, the crystal shape becomes a rectangle, while the unreacted regions retain the parallelogram shape. After partial conversion, when the reacted rectangular cells are located at the edges of the crystal and the unreacted unit cells occupy the middle, a distorted shape resembling a fluttering flag is obtained. Then, when the photoreaction is complete, the crystal shape changes to a perfect rectangle. Thus, the distinctive photomechanical shape change can be qualitatively understood by considering the changes in molecular packing that accompany the spatially heterogeneous photoreaction.

Conclusion

In this study, the behavior of ***p*-PDAMe** single crystals during photoreaction was thoroughly investigated, revealing both spatially heterogeneous photoreaction and a distinctive photomechanical shape change. The photoreaction was initiated at the crystal edges and progressed toward the center, driven by a positive cooperative effect and surface reactivity. This resulted in an unprecedented crystal shape transformation from a parallelogram to a fluttering flag-like structure, and finally to a rectangle. DFT calculations revealed the molecular packing changes due to the photoreaction. The method reported here may prove useful for determining the molecular packing after reactions of very small crystals with reduced crystallinity, which are challenging for conventional X-ray structural analysis. Based on the molecular packing changes and the spatially heterogeneous photoreaction, a mechanism for the distinctive photomechanical shape change was proposed. These findings illustrate the correlation between molecular-level packing changes and the macroscopic mechanical response in a single crystal. Furthermore, the heterogeneous distribution of photoproduct domains within the single crystal can give rise to unexpected shapes that may have future applications in photomechanical devices.

Supporting Information

The authors have cited additional references within the Supporting Information.[17,18]

Acknowledgements

This work was partly supported by JSPS KAKENHI Grant Numbers JP21KK0092, JP23K26619, JP24K01458, and JP24K21794 (D. K). D. K also acknowledges support from Iketani Science and Technology Foundation (Grant Number 0361012-A). C. J. B acknowledges support from the National Science Foundation, grant DMR-1810514. G. J. O. B. acknowledges funding from the U.S. Office of Naval Research grant N00014-24-1-2358 and supercomputer time from ACCESS (CHE110064).

Conflict of Interest

The authors declare no conflict of interest.

Data Availability Statement

The data that support the findings of this study are available in the supplementary material of this article.

Keywords: Organic Crystals · Photochemistry · Polymerization · Kinetics · Photomechanical Actuators

[1] a) B. L. Feringa, R. A. van Delden, N. Koumura, E. M. Geertsema, *Chem. Rev.* **2000**, *100*, 1789–1816; b) D. Kitagawa, K. Tanaka, S. Kobatake, *J. Mater. Chem. C* **2017**, *5*, 6210–6215; c) X. Dong, T. Guo, D. Kitagawa, S. Kobatake, P. Palffy-Muhoray, C. J. Bardeen, *Adv. Funct. Mater.* **2020**, *30*, 1902396; d) L. Li, P. Commins, M. B. Al-Handawi, D. P. Karothu, J. M. Halabi, S. Schramm, J. Weston, R. Rezgui, P. Naumov, *Chem. Sci.* **2019**, *10*, 7327–7332; e) L. Zhang, P. e. Naumov, X. Du, Z. Hu, J. Wang, *Adv. Mater.* **2017**; f) M. Irie, T. Fukaminato, K. Matsuda, S. Kobatake, *Chem. Rev.* **2014**, *114*, 12174–12277.

[2] T. J. White, *Photomechanical Materials, Composites, and Systems: Wireless Transduction of Light into Work*, John Wiley & Sons, **2017**.

[3] a) Y. Yu, M. Nakano, T. Ikeda, *Nature* **2003**, *425*, 145–145; b) S. Iamsaard, S. J. Aßhoff, B. Matt, T. Kudernac, J. J. Cornelissen, S. P. Fletcher, N. Katsonis, *Nat. Chem.* **2014**, *6*, 229–235.

[4] a) A. S. Kuenstler, K. D. Clark, J. Read de Alaniz, R. C. Hayward, *ACS Macro Lett.* **2020**, *9*, 902–909; b) C. D. Eisenbach, *Polymer* **1980**, *21*, 1175–1179.

[5] K. Iwaso, Y. Takashima, A. Harada, *Nat. Chem.* **2016**, *8*, 625–632.

[6] a) S. Kobatake, S. Takami, H. Muto, T. Ishikawa, M. Irie, *Nature* **2007**, *446*, 778–781; b) R. O. Al-Kaysi, A. M. Mueller, C. J. Bardeen, *J. Am. Chem. Soc.* **2006**, *128*, 15938–15939.

[7] a) P. Naumov, S. Chizhik, M. K. Panda, N. K. Nath, E. Boldyreva, *Chem. Rev.* **2015**, *115*, 12440–12490; b) M. Morimoto, M. Irie, *J. Am. Chem. Soc.* **2010**, *132*, 14172–14178; c) J. M. Halabi, E. Ahmed, S. Sofela, P. Naumov, *Proc. Natl. Acad. Sci. USA* **2021**, *118*.

[8] a) F. Tong, D. Kitagawa, X. Dong, S. Kobatake, C. J. Bardeen, *Nanoscale* **2018**, *10*, 3393–3398; b) T. Taniguchi, A. Kubota, T. Moritoki, T. Asahi, H. Koshima, *RSC Adv.* **2018**, *8*, 34314–34320; c) O. S. Bushuyev, A. Tomberg, T. Friscic, C. J. Barrett, *J. Am. Chem. Soc.* **2013**, *135*, 12556–12559; d) O. S. Bushuyev, T. A. Singleton, C. J. Barrett, *Adv. Mater.* **2013**, *25*, 1796–1800; e) H. Koshima, N. Ojima, *Dyes Pigm.* **2012**, *92*, 798–801; f) M. Tamaoki, D. Kitagawa, S. Kobatake, *Cryst. Growth Des.* **2021**, *21*, 3093–3099; g) F. Tong, M. Al-Haidar, L. Zhu, R. O. Al-Kaysi, C. J. Bardeen, *Chem. Commun.* **2019**, *55*, 3709–3712; h) J. M. Cole, J. d. J. Velazquez-Garcia, D. J. Gosztola, S. G. Wang, Y.-S. Chen, *Chem. Mater.* **2019**, *31*, 4927–4935; i) R. Medishetty, S. C. Sahoo, C. E. Mulijanto, P. Naumov, J. J. Vittal, *Chem. Mater.* **2015**, *27*, 1821–1829; j) P. Naumov, S. C. Sahoo, B. A. Zakharov, E. V. Boldyreva, *Angew. Chem. Int. Ed.* **2013**, *52*, 9990–9995; k) F. Tong, D. Kitagawa, I. Bushnak, R. O. Al-Kaysi, C. J. Bardeen, *Angew. Chem. Int. Ed.* **2021**, *60*, 2414–2423; l) A. K. Bartholomew, I. B. Stone, M. L. Steigerwald, T. H. Lambert, X. Roy, *J. Am. Chem. Soc.* **2022**, *144*, 16773–16777; m) K. Lam, V. Carta, M. Almtiri, I. Bushnak, I. Islam, R. O. Al-Kaysi, C. J. Bardeen, *J. Am. Chem. Soc.* **2024**, *146*, 18836–18840; n) B. B. Rath, J. J. Vittal, *J. Am. Chem. Soc.* **2020**, *142*, 20117–20123; o) H. Wang, P. Chen, Z. Wu, J. Zhao, J. Sun, R. Lu, *Angew. Chem. Int. Ed.* **2017**, *56*, 9463–9467; p) P. Naumov, S. C. Sahoo, B. A. Zakharov, E. V. Boldyreva, *Angew. Chem. Int. Ed.* **2013**, *52*, 9990–9995.

[9] a) A. Hirano, D. Kitagawa, S. Kobatake, *CrystEngComm* **2019**, *21*, 2495–2501; b) D. Kitagawa, H. Tsujioka, F. Tong, X. Dong, C. J. Bardeen, S. Kobatake, *J. Am. Chem. Soc.* **2018**, *140*, 4208–4212; c) A. Hirano, T. Hashimoto, D. Kitagawa, K. Kono, S. Kobatake, *Cryst. Growth Des.* **2017**, *17*, 4819–4825; d) D. Kitagawa, R. Tanaka, S. Kobatake, *Phys. Chem. Chem. Phys.* **2015**, *17*, 27300–27305.

[10] a) F. Tong, W. Xu, M. Al-Haidar, D. Kitagawa, R. O. Al-Kaysi, C. J. Bardeen, *Angew. Chem. Int. Ed.* **2018**, *57*, 7080–7084; b) R. O. Al-Kaysi, F. Tong, M. Al-Haidar, L. Zhu, C. J. Bardeen, *Chem. Commun.* **2017**, *53*, 2622–2625.

[11] a) D. Kitagawa, C. Iwaihara, H. Nishi, S. Kobatake, *Crystals* **2015**, *5*, 551–561; b) D. Kitagawa, S. Kobatake, *Photochem. Photobiol. Sci.* **2014**, *13*, 764–769; c) D. Kitagawa, S. Kobatake, *J. Phys. Chem. C* **2013**, *117*, 20887–20892.

[12] K. Morimoto, D. Kitagawa, H. Sotome, S. Ito, H. Miyasaka, S. Kobatake, *Angew. Chem. Int. Ed.* **2022**, *61*, e202212290.

[13] S. Kataoka, D. Kitagawa, H. Sotome, S. Ito, H. Miyasaka, C. J. Bardeen, S. Kobatake, *Chem. Sci.* **2024**, *15*, 13421–13428.

[14] H. Nakanishi, M. Hasegawa, Y. Sasada, *J. Polym. Sci. Polym. Phys. Ed.* **1977**, *15*, 173–191.

[15] K. Ueno, H. Nakanishi, M. Hasegawa, Y. Sasada, *Acta Crystallogr. Sect. B* **1978**, *34*, 2034–2035.

[16] a) C. J. Perry, G. J. O. Beran, *Cryst. Growth Des.* **2023**, *23*, 8352–8360; b) C. J. Cook, C. J. Perry, G. J. O. Beran, *J. Phys. Chem. Lett.* **2023**, *14*, 6823–6831; c) C. J. Cook, W. Li, B. F. Lui, T. J. Gately, R. O. Al-Kaysi, L. J. Mueller, C. J. Bardeen, G. J. O. Beran, *Chem. Sci.* **2023**, *14*, 937–949.

[17] a) A. D. Becke, *J. Chem. Phys.* **1986**, *85*, 7184–7187; b) J. P. Perdew, K. Burke, M. Ernzerhof, *Phys. Rev. Lett.* **1996**, *77*, 3865–3868.

[18] A. Otero-de-la-Roza, E. R. Johnson, *J. Chem. Phys.* **2012**, *136*, 174109.

Manuscript received: October 18, 2024
Accepted manuscript online: November 19, 2024
Version of record online: December 2, 2024